

RELIABILITY MODELING IN SOME ELASTIC STABILITY PROBLEMS VIA THE GENERALIZED STOCHASTIC FINITE ELEMENT METHOD

M. KAMIŃSKI¹, P. ŚWITA²

The main idea of this work is to demonstrate an application of the generalized perturbation-based Stochastic Finite Element Method for a determination of the reliability indicators concerning elastic stability for a certain spectrum of the civil engineering structures. The reliability indicator is provided after the Eurocode according to the First Order Reliability Method, and computed using the higher order Taylor expansions with random coefficients. Computational implementation provided by the hybrid usage of the FEM system ROBOT and the computer algebra system MAPLE enables for reliability analysis of the critical forces in the most popular civil engineering structures like simple Euler beam, 2 and 3D single and multi-span steel frames, as well as polyethylene underground cylindrical shell. A contrast of the perturbation-based numerical approach with the Monte-Carlo simulation technique for the entire variability of the input random dispersion included into the Euler problem demonstrates the probabilistic efficiency of the perturbation method proposed.

Key words: stability analysis; perturbation method; Stochastic Finite Element Method; Response Function Method; reliability indicator; elastic buckling.

1. INTRODUCTION

As it is widely known, the computational stability analysis is especially important in the area of the steel and/or aluminium structures, where the structural elements are usually very slender. Therefore, the critical load magnitude and the additional limit state must be evaluated to optimally design the structure with the given geometry and spatial distribution of the components. This optimization problem has to be solved with the use of verification of reliability indicator according to the general rules provided by Eurocode appendices [1]; this indicator consists of the expected values and standard deviations of the admissible (now critical) and maximum load values, which need to be pre-calculated first. Because the Eurocode gives no direct general algorithm of how to calculate this indicator and the component probabilistic moments, this elaboration

¹ Professor, Chair of Steel Structures, Department of Structural Mechanics Faculty of Civil Engineering, Architecture and Environmental Engineering Technical University of Łódź, Poland. e-mail: Marcin.Kaminski@p.lodz.pl

² Ph.D. Student, Chair of Steel Structures, Department of Structural Mechanics Faculty of Civil Engineering, Architecture and Environmental Engineering Technical University of Łódź, Poland.

contains a relatively brief description of how to proceed in this case and what can be expected in these structures (both steel and composite). Of course, there are plenty available well-established methods of the first, second, as well as higher order methods leading to a determination of the reliability indices or, directly, the probability of failure. They depend strongly on the shape of the boundary between safe and unsafe regions in the additional parametric space [2]. We strictly follow the First Order Reliability Method to discover and discuss the consequences of an application of the regulations of Eurocode in engineering practice assuming that the designers have an access to the probabilistic algorithms and computer programs.

We employ two alternative probabilistic methodologies available for stability analysis [3,4] – namely Monte-Carlo simulation, and the generalized stochastic perturbation – to determine reliability indicators for the Euler problem, 2 and 3D models of the same single span steel frame, for 2D model of the multi-span and multi-storey steel frame, as well as for the underground cylindrical composite shell structure. An application of the generalized version of the stochastic perturbation technique follows the fact that the second order second moment (SOSM) implementation of this method was restricted to the input coefficients of variation smaller than $\alpha=0.15$ [5]. The response function method implemented into the computer algebra system MAPLE [17] is employed to calculate partial derivatives of the critical and maximum compressive forces with respect to two separate input random variables – Young modulus and cross-sectional axis inertia moment. The structural analyses using the Finite Element Method are carried out for both stability and static problems thanks to the commercial engineering package ROBOT [18] and the response functions are computed via several solutions with slightly modified input parameters, which are to be treated as random quantities. We calculate twice the reliability indicators for those structures as the function of input coefficient of variation α and compare with the admissible values of indicator β taken directly from Eurocode. This is done to find an interrelation $\beta = \beta(\alpha)$ and, furthermore, to determine the maximum input random dispersion of those two input random parameters equivalent to the specific reliability class according to Eurocode demands. The most common result is that the higher input random dispersion, the smaller overall reliability indicator, and this result is compliant rather perfectly with the engineering intuition in this matter. The stochastic perturbation-based method proposed in this paper is characterized by essentially smaller computational time cost in comparison to the Monte-Carlo simulation, comparable rather to the multiple deterministic solutions, and having almost the same efficiency as the additional simulation-based estimators for the reliability indicators. Once T denotes the time of deterministic FEM problem solution, the simulation-based analysis is closer to $10^4 \times T$, while the methodology proposed results in not more than $15 \times T$ excluding common deterministic FEM discretization effort. The model presented in the paper is rather an introductory step into the full probabilistic stability analysis of the steel thin-walled profiles – the next step would consist in evaluation of the critical moments under the combined bending-torsional load, and final comparison with the maximum moments calculated for the structural

members. We need to emphasize that while the randomization of the Young modulus strictly follows the experimental statistics, the uncertainty in element thickness or inertia moments may simulate the effect of their corrosion, however further calibration with corrosion statistics may be needed to provide time correlation of the results computed here.

2. THE GENERALIZED STOCHASTIC FINITE ELEMENT METHOD

Let us introduce the random variable $b \equiv b(\omega)$ and its probability density function as $p(b)$, where ω (stating frequently for the random event in probability theory) denotes that their function belongs to the additional probability space. We use Gaussian probability spaces for this purpose truncated to the physically admissible values, like positive for the Young modulus etc. Then, the expected values, as well as their central m th probabilistic moments are defined as [5,6]

$$(2.1) \quad E[b] \equiv b^0 = \int_{-\infty}^{+\infty} b p(b) db,$$

and

$$(2.2) \quad \mu_m(b) = \int_{-\infty}^{+\infty} (b - E[b])^m p(b) db.$$

The basic idea of this stochastic perturbation approach is to expand all the input variables and all the state functions of the considered problem via Taylor series about the additional expected values using the parameter $\varepsilon > 0$. In the case of random critical force P_{cr} depending on some random input quantity b , the following expression is employed [6]:

$$(2.3) \quad P_{cr} = P_{cr}^0 + \sum_{n=1}^{\infty} \frac{1}{n!} \varepsilon^n \frac{\partial^n P_{cr}}{\partial b^n} (\Delta b)^n,$$

where

$$(2.4) \quad \varepsilon \Delta b = \varepsilon (b - b^0)$$

is the first variation of b around its expected value b^0 . We will derive the expected value for the critical force P_{cr} in view of above expansion as

$$(2.5) \quad E[P_{cr}] = \int_{-\infty}^{+\infty} P_{cr}(b) p(b) db = \int_{-\infty}^{+\infty} \left(P_{cr}^0 + \sum_{n=1}^{\infty} \frac{1}{n!} \varepsilon^n \frac{\partial^n P_{cr}}{\partial b^n} \Delta b^n \right) p(b) db$$

Let us remind that this power expansion is valid only if the state function is analytic in ε , the series converge and, therefore, any criteria of convergence should include the magnitude of the perturbation parameter; perturbation parameter is usually taken simply as equal to 1 in engineering computations. Contrary to most of the previous analyses in this area (see [5], for instance), now the quantity ε is treated as the expansion parameter in further analysis, so that it is included explicitly in all further derivations demanding analytical expressions.

From the numerical point of view, the expansion provided by formula (2.3) is carried out for the summation over the finite number of components, whereas the integral given in definition (2.5) is never calculated with infinite limits – usually it has lower and upper bounds driven by physical meaning of the specific parameter, or just the experimental works. Having Gaussian input in the form of $b(\omega)$ or another symmetric probability distribution function, one can show that

$$(2.6) \quad E[P_{cr}] = P_{cr}(b^0) + \frac{1}{2}\varepsilon^2 \frac{\partial^2 P_{cr}(b^0)}{\partial b^2} \mu_2(b^0) + \frac{1}{2m!} \varepsilon^{2m} \frac{\partial^{2m} P_{cr}(b^0)}{\partial b^{2m}} \mu_{2m}(b^0) + \dots$$

This expected value can be calculated analytically or symbolically computed only if it is given as some analytical function of the random input parameter b . Computational implementation of the symbolic calculus programs (with automatic partial differentiation of even complex real functions), combined with powerful visualization of probabilistic output moments, ensures the fastest solution of such problems. Further, thanks to such a series representation of the random output, any desired efficiency of the expected values, as well as higher probabilistic moments, can be achieved by an appropriate choice of the expansion length and some additional correction available in the parameter ε , which depends on the input probability density function (PDF) type, interrelations between the probabilistic moments, acceptable error of the computations etc. This choice can be made by the comparative studies with sufficiently long (almost infinite) series of Monte-Carlo simulations or theoretical results obtained from the direct symbolic integration. Similar considerations lead to the 6th order expressions for a variance; there holds

(2.7)

$$\begin{aligned} \text{Var}(P_{cr}(b)) = & \varepsilon^2 \mu_2(b) \left(\frac{\partial P_{cr}(b^0)}{\partial b} \right)^2 \\ & + \varepsilon^4 \mu_4(b) \left(\frac{1}{4} \left(\frac{\partial^2 P_{cr}(b^0)}{\partial b^2} \right)^2 + \frac{2}{3!} \frac{\partial P_{cr}(b^0)}{\partial b} \frac{\partial^3 P_{cr}(b^0)}{\partial b^3} \right) \\ & + \varepsilon^6 \mu_6(b) \left(\left(\frac{1}{3!} \right)^2 \left(\frac{\partial^3 P_{cr}(b^0)}{\partial b^3} \right)^2 + \frac{1}{4!} \frac{\partial^2 P_{cr}(b^0)}{\partial b^2} \frac{\partial^4 P_{cr}(b^0)}{\partial b^4} + \frac{2}{5!} \frac{\partial P_{cr}(b^0)}{\partial b} \frac{\partial^5 P_{cr}(b^0)}{\partial b^5} \right) \end{aligned}$$

Let us mention that it is necessary to insert the relevant central probabilistic moments of the input random variable in each of those equations to get the algebraic form convenient for symbolic computations. A recursive derivation of the particular perturbation order equilibrium equations can be powerful in conjunction with symbolic packages with automatic differentiation tools only; it can potentially extend the area of stochastic perturbation technique applications in computational physics and engineering outside the random processes with small dispersion about their expected values. Hence, there is no need to implement directly exact formulas for the particular n th order equations extracted from the perturbation – they can be symbolically generated in the system MAPLE, as it is done here, and next converted to the FORTRAN source codes of the additional computer software. Finally, it should be emphasized that the random input variables must express here the uncertainty in space or in time, separately.

Having determined the first two probabilistic moments of the critical force one may calculate the Cornell reliability indicator using the limit function g according to the following formula:

$$(2.8) \quad \beta = \frac{E[g]}{\sigma(g)} = \frac{E[R-E]}{\sigma(R-E)} = \frac{E[R] - E[E]}{\sqrt{\text{Var}(R-E)}} = \frac{E[R] - E[E]}{\sqrt{\text{Var}(R) + \text{Var}(E)}}$$

where R denotes the structural capacity, while E stands for the structural response. Then, the failure probability P_f is found from the relation

$$(2.9) \quad P_f = \Phi(-\beta)$$

where Φ is a probability density function of the standardized Gaussian distribution. The minimal values of this indicator are specific for the three reliability classes and given in Eurocode with respect to two different time periods of the structure exploitation – at the very beginning of this exploitation (after a year) and at the average designed time of reliable exploitation (50 years) – see table 1. Computational analysis provided in Section 4 shows a variability of the reliability indices for the popular structures contrasted with those specific limits. We look for the admissible input random dispersion of the given random variables to keep the reliability indicator above the additional limit and to fulfill the durability condition.

Table 1

Proposed minima values of the reliability indicator.
Proponowane wartości minimalne wskaźników niezawodności

Reliability class	Minimal values of β	
	1 year period	50 years period
RC3	5,2 (β_1)	4,3 (β_4)
RC2	4,7 (β_2)	3,8 (β_5)
RC1	4,2 (β_3)	3,3 (β_6)

3. ELASTIC STABILITY BY THE FINITE ELEMENT METHOD AND THE RESPONSE FUNCTIONS

The Finite Element Method (FEM) discretization is described here in terms of the Response Function Method (RFM) convenient for further solution to the structural problem exhibiting uncertainty in some design parameter. According to the previous work [6], we perform a sequence of the deterministic solutions, where the value of input random parameter is treated as deterministically varying around its mean value – for the brevity of presentation, the new index α is used here to expose this variability. This symbol is introduced as the lower index in brackets in all FEM equations to underline that no summation applies here with respect to this new index. The specific character of the RFM approach is that the variability of all FEM matrices and vectors holds true except to the shape functions and their derivatives. Let us consider the linear elastic prismatic beam ($E_{(\alpha)}$ – Young modulus, $l_{(\alpha)}$ – length, $A_{(\alpha)}$ – cross sectional area, $F_{(\alpha)}$ – axial force) element with two nodes indexed by i and j at its ends. Then, the deformation energy of the finite element idealizing elastic behavior of the simple prismatic bar is introduced for 3D Cartesian system as [7,8]

$$(3.1) \quad U^{(\alpha)} = \frac{1}{2} \mathbf{q}_{1 \times 6(\alpha)}^T \mathbf{k}_{6 \times 6(\alpha)}^{(s)} \mathbf{q}_{6 \times 1(\alpha)} + \frac{1}{2} \mathbf{q}_{1 \times 6(\alpha)}^T \mathbf{k}_{6 \times 6(\alpha)}^{(\sigma)} \mathbf{q}_{6 \times 1(\alpha)}$$

where $\mathbf{q}_{(\alpha)}$ is the displacement vector of the nodes

$$(3.2) \quad \mathbf{q}_{(\alpha)} = \{u_{x(\alpha)}^{(i)}, u_{y(\alpha)}^{(i)}, u_{z(\alpha)}^{(i)}, u_{x(\alpha)}^{(j)}, u_{y(\alpha)}^{(j)}, u_{z(\alpha)}^{(j)}\},$$

$\mathbf{k}_{4 \times 4(\alpha)}^{(s)}$ is the elemental elastic stiffness matrix introduced as

$$(3.3) \quad \mathbf{k}_{6 \times 6(\alpha)}^{(s)} = \frac{E_{(\alpha)} A_{(\alpha)}}{l_{(\alpha)}} \begin{bmatrix} 1 & 0 & 0 & -1 & 0 & 0 \\ 0 & 0 & 0 & 0 & 0 & 0 \\ 0 & 0 & 0 & 0 & 0 & 0 \\ -1 & 0 & 0 & 1 & 0 & 0 \\ 0 & 0 & 0 & 0 & 0 & 0 \\ 0 & 0 & 0 & 0 & 0 & 0 \end{bmatrix}$$

and $\mathbf{k}_{6 \times 6(\alpha)}^{(\sigma)}$ – the geometric stiffness matrix of this finite element

$$(3.4) \quad \mathbf{k}_{6 \times 6(\alpha)}^{(\sigma)} = \frac{F_{(\alpha)}}{l_{(\alpha)}} \begin{bmatrix} 0 & 0 & 0 & 0 & 0 & 0 \\ 0 & 0 & 0 & 0 & 0 & 0 \\ 0 & 0 & 1 & 0 & 0 & -1 \\ 0 & 0 & 0 & 0 & 0 & 0 \\ 0 & 0 & 0 & 0 & 0 & 0 \\ 0 & 0 & -1 & 0 & 0 & 1 \end{bmatrix}$$

Stability analysis of the planar or spatial frames as well as plates or shells demands the interchange of this matrix with the one convenient for the structural element being modeled. So that, the potential energy for this finite element may be expressed as

$$(3.5) \quad J_P^{(\alpha)} = \frac{1}{2} \mathbf{q}_{(\alpha)}^T \left(\mathbf{k}_{(\alpha)}^{(s)} + \mathbf{k}_{(\alpha)}^{(\sigma)} \right) \mathbf{q}_{(\alpha)} - \mathbf{R}_{(\alpha)}^T \mathbf{q}_{(\alpha)}$$

the minimization of which with respect to the generalized displacement vector leads to

$$(3.6) \quad \left(\mathbf{k}_{(\alpha)}^{(s)} + \mathbf{k}_{(\alpha)}^{(\sigma)} \right) \mathbf{q}_{(\alpha)} = \mathbf{R}_{(\alpha)}$$

All these series of elemental stiffness matrices, together with the corresponding series of generalized displacement vectors, are then linked together into the corresponding series of global matrices and vectors following traditional algorithm of the FEM. The discrete stability equation rewritten for the entire system is

$$(3.7) \quad \left(\mathbf{K}_{(\alpha)}^{(s)} + \lambda_{(\alpha)} \mathbf{K}_{(\alpha)}^{(\sigma)} \left(\hat{F}_{(\alpha)} \right) \right) \mathbf{r}_{(\alpha)} = \lambda_{(\alpha)} \hat{\mathbf{R}}_{(\alpha)}$$

where $\mathbf{K}_{(\alpha)}^{(\sigma)} \left(\hat{F}_{(\alpha)} \right)$ is the series of geometric stiffness matrices, $\mathbf{K}_{(\alpha)}^{(s)}$ is the series of the elastic stiffness matrices, the given loading series $\mathbf{R}_{(\alpha)}$ has proportional character to $\lambda_{(\alpha)} \hat{\mathbf{R}}_{(\alpha)}$, where $\lambda_{(\alpha)}$ is the loading factor series and $\hat{\mathbf{R}}_{(\alpha)}$ is some loading. Further, the distribution of internal forces $\hat{F}_{(\alpha)}$ is equivalent to the load $\hat{\mathbf{R}}_{(\alpha)}$ and displacement $\mathbf{r}_{(\alpha)}$ is equivalent to the load $\lambda_{(\alpha)} \hat{\mathbf{R}}_{(\alpha)}$. We determine the values of $\lambda_{(\alpha)}$ from the following condition:

$$(3.8) \quad \begin{cases} \left(\mathbf{K}_{(\alpha)}^{(s)} + \lambda_{(\alpha)} \mathbf{K}_{(\alpha)}^{(\sigma)} \left(\hat{F}_{(\alpha)} \right) \right) \mathbf{r}_{1(\alpha)} = \lambda_{(\alpha)} \hat{\mathbf{R}}_{(\alpha)} \\ \left(\mathbf{K}_{(\alpha)}^{(s)} + \lambda_{(\alpha)} \mathbf{K}_{(\alpha)}^{(\sigma)} \left(\hat{F}_{(\alpha)} \right) \right) \mathbf{r}_{2(\alpha)} = \lambda_{(\alpha)} \hat{\mathbf{R}}_{(\alpha)} \end{cases}, \quad \mathbf{r}_{1(\alpha)} \neq \mathbf{r}_{2(\alpha)}, \mathbf{r}_{1(\alpha)} - \mathbf{r}_{2(\alpha)} = \mathbf{v}_{(\alpha)}$$

so that we obtain the basic algebraic equation series representing the elastic stability

$$(3.9) \quad \left(\mathbf{K}_{(\alpha)}^{(s)} + \lambda_{(\alpha)} \mathbf{K}_{(\alpha)}^{(\sigma)} \left(\hat{F}_{(\alpha)} \right) \right) \mathbf{v}_{(\alpha)} = 0$$

Therefore, the basic condition that one can get for the critical value $\lambda_{(\alpha)} = \lambda_{cr(\alpha)}$ and for critical load $\mathbf{R}_{cr(\alpha)} = \lambda_{cr(\alpha)} \hat{\mathbf{R}}_{(\alpha)}$ is the following one:

$$(3.10) \quad \det \left(\mathbf{K}_{(\alpha)}^{(s)} + \lambda_{(\alpha)} \mathbf{K}_{(\alpha)}^{(\sigma)} \left(\hat{F}_{(\alpha)} \right) \right) = 0$$

The key issue of this approach is the polynomial representation of the critical value λ_{cr} with respect to the input random variable b , which is proposed for all real values indexed here by m as [9]

$$(3.11) \quad \lambda_{cr}^{(m)} = D_{mk} b^k$$

The coefficients D_{mk} are determined numerically from several deterministic solutions to the original stability matrix equation with random parameter value varying around its mean value in the interval $b = [b^0 - \Delta b, b^0 + \Delta b]$ (Young modulus, for instance) or, following some engineering aspects, over some finite set of the specific discrete values (like inertia moments for the existing steel profiles). Then, the technique of nonlinear least square fitting is employed to find out the coefficients of the response polynomial, which is realized here using symbolic analysis implemented in the computer algebra system MAPLE. Finally, both in analytical way, the partial derivatives of the response functions are derived by using the formula:

$$(3.12) \quad \frac{\partial^k \lambda_{cr}^{(m)}}{\partial b^k} = \prod_{j=1}^k (n-j) D_{m1} b^{n-k} + \prod_{j=2}^k (n-j) D_{m2} b^{n-(k+1)} + \dots + D_{m, n-k}.$$

The Response Function Method in its global formulation is used here since the critical force or pressure have both global character for the entire structure being examined; more subtle local formulation is advised for the random fields of structural response like displacements, temperatures or stresses. When one uses the following expansion as it is proposed for most of the computational tests below

$$(3.13) \quad \lambda_{(cr)} = \sum_{k=0}^9 D_k b^k$$

then the expected values of the critical force derived symbolically for the 10th order approach is represented by the following formula:

$$(3.14) \quad \begin{aligned} E[\lambda_{(cr)}] = & D_0 + 4374 \alpha^8 \varepsilon^8 (3,6288 D_9 b + 40320 D_8) + \\ & + 972 \alpha^6 \varepsilon^6 (60480 D_9 b^3 + 20160 D_8 b^2 + 5040 D_7 b + 720 D_6) + \\ & + 162 \alpha^4 \varepsilon^4 (3024 D_9 b^5 + 1680 D_8 b^4 + 840 D_7 b^3 + 360 D_6 b^2 + 120 D_5 b + 24 D_4) + \\ & + 18 \alpha^2 \varepsilon^2 (72 D_9 b^7 + 56 D_8 b^6 + 42 D_7 b^5 + 30 D_6 b^4 + 20 D_5 b^3 + 12 D_4 b^2 + 6 D_3 b + 2 D_2) \end{aligned}$$

The variances, even according to the sixth order, have essentially more complex formula

$$(3.15) \quad \begin{aligned} \mu_2(\lambda_{(cr)}) = & 36 \alpha^2 \varepsilon^2 (9 D_9 b^8 + 8 D_8 b^7 + 7 D_7 b^6 + 6 D_6 b^5 + 5 D_5 b^4 + 4 D_4 b^3 + 3 D_3 b^2 + 2 D_2 b + D_1)^2 \\ & + \frac{3888}{4} \alpha^4 \varepsilon^4 (72 D_9 b^7 + 56 D_8 b^6 + 42 D_7 b^5 + 30 D_6 b^4 + 20 D_5 b^3 + 12 D_4 b^2 + 6 D_3 b + 2 D_2)^2 \\ & + \frac{3888}{3} \alpha^4 \varepsilon^4 (9 D_9 b^8 + 8 D_8 b^7 + 7 D_7 b^6 + 6 D_6 b^5 + 5 D_5 b^4 + 4 D_4 b^3 + 3 D_3 b^2 + 2 D_2 b + D_1) \times \\ & \quad \times (504 D_9 b^6 + 336 D_8 b^5 + 210 D_7 b^4 + 120 D_6 b^3 + 60 D_5 b^2 + 24 D_4 b + 6 D_3) \\ & + 6,998 \frac{\alpha^6 \varepsilon^6}{36} (504 D_9 b^6 + 336 D_8 b^5 + 210 D_7 b^4 + 120 D_6 b^3 + 60 D_5 b^2 + 24 D_4 b + 6 D_3) + \end{aligned}$$

$$\begin{aligned}
& +6,998 \frac{\alpha^6 \varepsilon^6}{24} (3024D_9b^5 + 1680D_8b^4 + 840D_7b^3 + 360D_6b^2 + 120D_5b + 24D_4) \times \\
& \quad \times (72D_9b^7 + 56D_8b^6 + 42D_7b^5 + 30D_6b^4 + 20D_5b^3 + 12D_4b^2 + 6D_3b + 2D_2) + \\
& +6,998 \frac{\alpha^6 \varepsilon^6}{60} (15120D_9b^4 + 6720D_8b^3 + 2520D_7b^2 + 720D_6b + 120D_5) \times \\
& \quad \times (9D_9b^8 + 8D_8b^7 + 7D_7b^6 + 6D_6b^5 + 5D_5b^4 + 4D_4b^3 + 3D_3b^2 + 2D_2b + D_1)
\end{aligned}$$

Determination of probabilistic moments for the maximum load proceeds quite similarly; we solve for the displacements vector set $\mathbf{q}_{(\alpha)}$ from the matrix equilibrium equations:

$$(3.16) \quad \mathbf{K}_{(\alpha)} \mathbf{q}_{(\alpha)} = \mathbf{Q}_{(\alpha)}$$

where $\mathbf{K}_{(\alpha)}$ denotes traditional stiffness matrix of the system and where $\mathbf{Q}_{(\alpha)}$ is equivalent to the external loads vector. However now, the discrete response functions are applied, which means that for each degree of freedom $\beta = 1, \dots, N$ we provide separately a polynomial expansion of the following character:

$$(3.17) \quad q_\beta = \hat{D}_{\beta m} b^m$$

so that the coefficients $\hat{D}_{\beta m}$ (for $m=1, \dots, M$, M – total number of the RFM trial points) are to be computed from node to node separately, which enlarges the computational time consumption in the analysis. Finally, the strain and stress tensors components are computed here using the following polynomial approximations:

$$(3.18) \quad \varepsilon_{ij} = B_{ij\beta} q_\beta = B_{ij\beta} \hat{D}_{\beta m} b^m$$

and

$$(3.19) \quad \sigma_{kl} = C_{klij} \varepsilon_{ij} = C_{klij} B_{ij\beta} q_\beta = C_{klij} B_{ij\beta} \hat{D}_{\beta m} b^m$$

Basic probabilistic moments of the vector q_β and the tensors ε_{ij} , σ_{kl} may be relatively easily derived by replacing in the expanded formulas (3.14-3.15) D_m with $\hat{D}_{\beta m}$ and by inserting the additional multipliers like $B_{ij\beta}$ and/or $C_{klij} B_{ij\beta}$ for all necessary components.

4. COMPUTATIONAL ANALYSIS

4.1. NUMERICAL ANALYSIS OF THE EULER PROBLEM

The first numerical example is devoted to the comparison of the reliability indicator determined by using the Monte-Carlo simulation [10] and, alternatively, via the generalized stochastic perturbation technique described above. The last approach uses 10^{th} order expansion for a determination of the expected values and 6^{th} order – for

the variances calculation, while the Monte-Carlo simulation analysis has been provided by using crude sampling with the length of $N=10000$ samples in the program MAPLE. The studied case is the linear elastic and statistically homogeneous beam with the constant cross-section of HEB 300, the length of $L=7,0$ m with the randomized Young modulus typical for the stainless steel S355. Its expected value is equal to $E[E]=210$ GPa, whereas its standard deviation (showing the random dispersion) is the additional input parameter of this study (given in all next figures as the coefficient of variation). Such a large dispersion, $\alpha \in [0,0, 0,45]$ is enormously large for the structural steels at the very beginning of the exploitation time, however it may happen for the structures subjected to the extended corrosion processes, and that is why it still remains interesting. The FEM model is built up with 1000 linear finite elements to be compared against the well-known analytical solution available for the simulation approach. The trial points coming from both numerical methods are marked with the diamonds (see Fig. 1) and the polynomial approximations for those data sets are applied – it is apparent that the functions obtained are continuous, smooth and convex everywhere, nonlinearly decreasing to theoretical value 0 obtained for $\alpha \rightarrow \infty$. Nevertheless, it is seen that the final reliability indicator is significantly sensitive to the variations of input coefficient of variations and even small change within α may result in the apparent change of this indicator. It needs to be mentioned that the response function is determined from

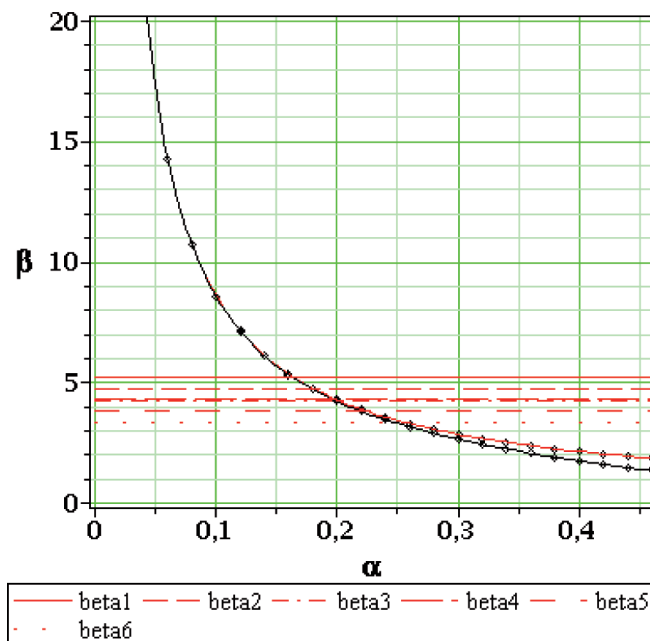


Fig. 1. Reliability indices for the Euler problem.
Rys. 1. Wskaźniki niezawodności w zadaniu Eulera

the numerical experiments provided for $E=E[E](1\pm 0.4)$ and the equidistant set of trial points within this interval; the same discretization is used in the next computational experiments also.

Figure 1 shows the reliability indicator contrasted with 6 limit values mentioned in Eurocode – upper curve demonstrates here the simulation-based results, while lower one – those obtained from the stochastic perturbation analysis. It is apparent that practically they return the same results for the input coefficient of variation $\alpha \in [0.0, 0.2]$. As one may expect, the higher input random dispersion (higher uncertainty of the given design parameter), the smaller reliability indicator and, at the same time, the larger probability of failure. The third observation is that the entire structure is above any reliability limit until $\alpha = 0.15$, which is relatively large value, because this parameter is usually less than 0.10 for the stainless steels at the production stage; this result is quite independent from the reliability class provided according to Eurocode [1]. It is confirmed by those computations that the reliability condition is first violated for β equivalent to the one year period and, after that, for 50 years period for all reliability classes. One may relatively easy repeat those two techniques to randomize the other analytical results available in the classical stability theories [11,12].

4.2. 2D AND 3D MODELS FOR THE SINGLE-SPAN STEEL FRAME STRUCTURE

The main purpose of the second computational example was to make a comparison between 2 (Fig. 2) and 3 dimensional models (Fig. 3) of the same steel frame structure

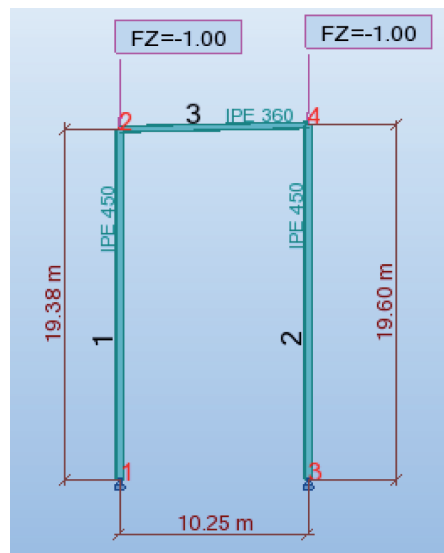


Fig. 2. 2D FEM model of the steel frame.
Rys. 2. Dwuwymiarowy model ramy stalowej

made of S235 in the context of the resulting variability of reliability indicator. The subject of this study is the magnitude of the critical loading introduced by the vertical unit forces (given in kN) applied at two midpoint columns. The key issue here is the influence of the model quality on the final values of the basic reliability indicators. Two polynomial approximations have been numerically developed using the FEM system ROBOT, as well as the computer algebra system MAPLE, v. 13, to finally determine the reliability indicators varying together with the input coefficient of variation for 2D model (Fig. 4), as well as for the 3D model (Fig. 5).

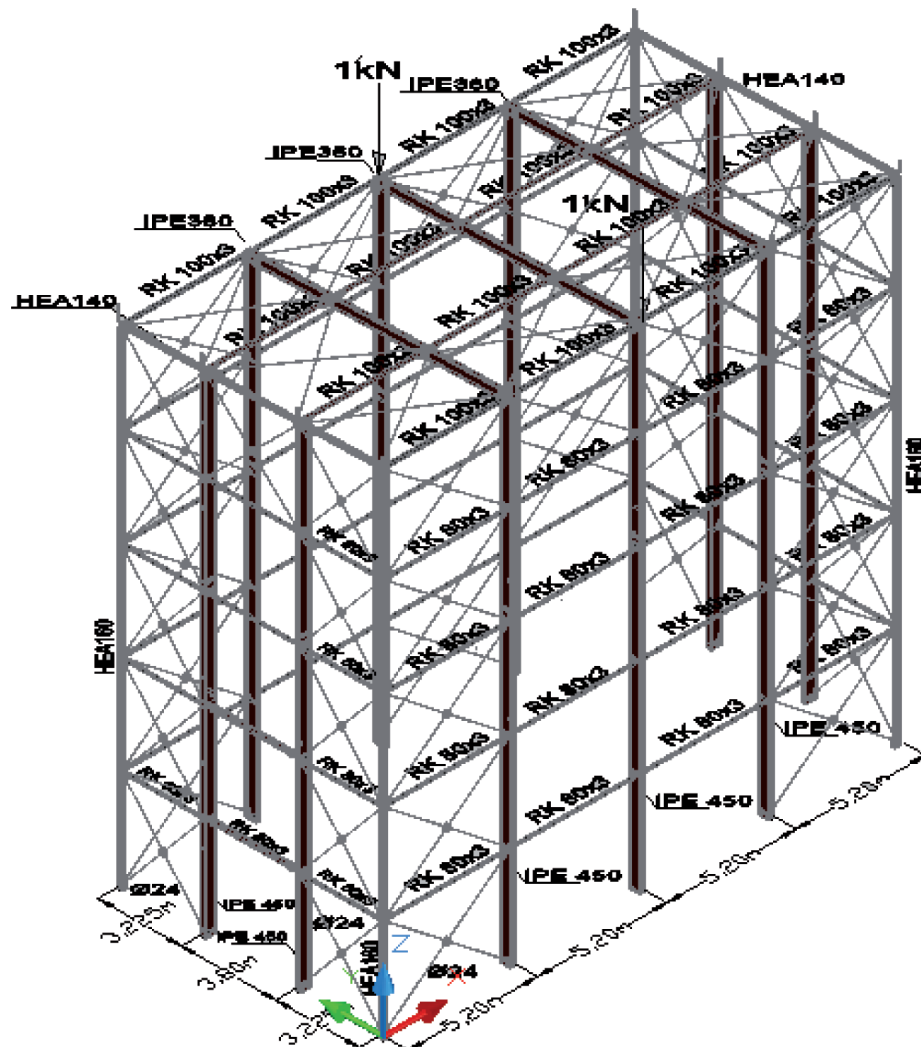


Fig. 3. 3D FEM model of the steel frame.
Rys. 3. Trójwymiarowy model ramy stalowej

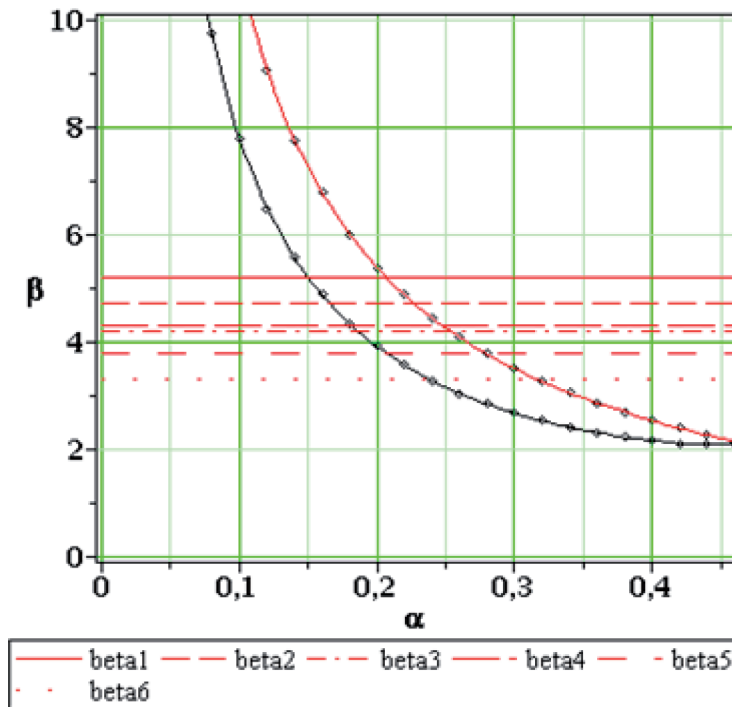


Fig. 4. Reliability indices for the 2D FEM model of the steel frame.

Rys. 4. Wskaźniki niezawodności dla dwuwymiarowego modelu ramy stalowej

Now we have chosen separately the Young modulus of the steel, as well as the principal inertia moment of the columns as the input Gaussian random variables. Comparison of Fig. 4 and 5 shows first that the indicators β start from the maximum reached at the very beginning of the exploitation time (equivalent to α close to 0), and tend to some minimal values at the end of the safe exploitation time (for the increasing values of α). Further, they are significantly larger for randomized inertia moment (upper curves) than for the Young modulus. Uncertainty of the last variable leads to the safe exploitation for all reliability classes until $\alpha(E) \leq 0.15$ (in 2D model) and until $\alpha(E) \leq 0.13$ (in 3D model). Somewhat inverse relation is noticed for $J=J(\omega)$ – the unconditional safety holds true for $\alpha(J) \leq 0.2$ (in planar mode) and for $\alpha(J) \leq 0.32$ (spatial structure). Quite similarly to the previous case study we obtain quite smooth and convex reliability curves. It is very interesting (see Fig. 4) that the final value of the indicator β is the same in 2D model (about 2) for input coefficients of variation of both input variables equal to about 0.46. Neglecting the reliability class of the structure, the differences between α equivalent to β_1 and β_6 each time correspond to an increase of this coefficient by about 0.10. This is the intermediate safety level measure for most of the engineering structures designed safely according to the zeroth order methods.

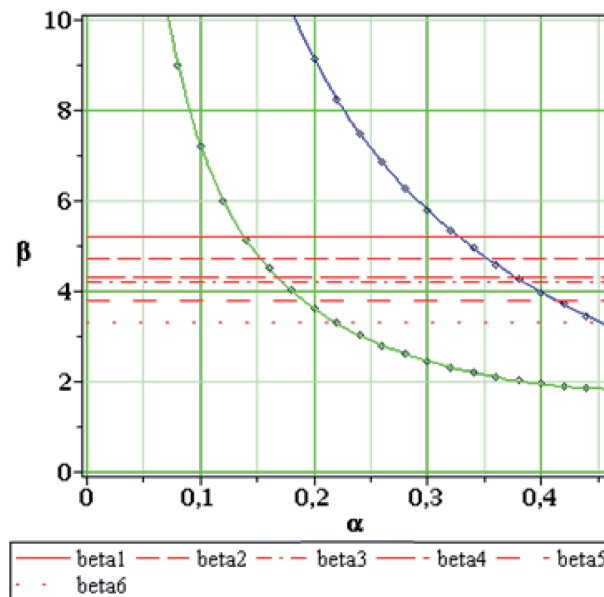


Fig. 5. Reliability indices for the 3D FEM model of the steel frame.
Rys. 5. Wskaźniki niezawodności dla trójwymiarowego modelu ramy stalowej

4.3. 2D MODEL OF THE MULTI-SPAN STEEL FRAME STRUCTURE

The next series of numerical experiments deals with the probabilistic stability analysis for the simply supported multi-span structure, discretized by using linear beam elements according to the static scheme presented in Fig. 6. Once more the inertia moment and Young modulus are the Gaussian input random variables defined uniquely by their expected values and coefficients of variation, used further as the additional study parameter. The polynomial approximation of the response function – magnitude of the critical load (P_{cr}) vs. inertia moment (J) – is given in Fig. 7. The subdivision of the variability interval for this random input variable is non-uniform, and the final form of this response function is smooth, concave, with no local oscillations. Let us mention that the usage of the symbolic least squares fitting procedures enables further systematic corrections of the local weights until the satisfactory and efficient approximation is obtained. After Euler formula, one can suppose that the higher inertia moment, the larger critical force magnitude, and it is reflected well on Fig. 7, however now, this interrelation, although preserving directional proportionality, is nonlinear unlike in the Euler formula. Let us finally note that the analyzed steel frame was modeled by using fully rigid connections between all the structural members, but in fact they exhibit some semi-rigid behavior, which also influences in some way its stability and needs to be taken into account in further reliability analysis.

Final evaluation of the reliability indicator with respect to two input parameters and their coefficients of variation is given in Fig. 8. Once more we introduce the limit

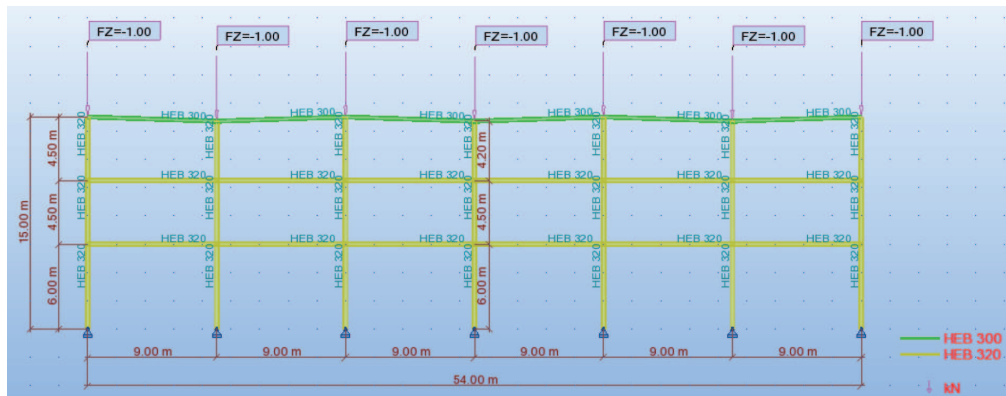


Fig. 6. FEM model of the multi-span steel frame.
Rys. 6. Model MES wieloprzęsłowej ramy stalowej

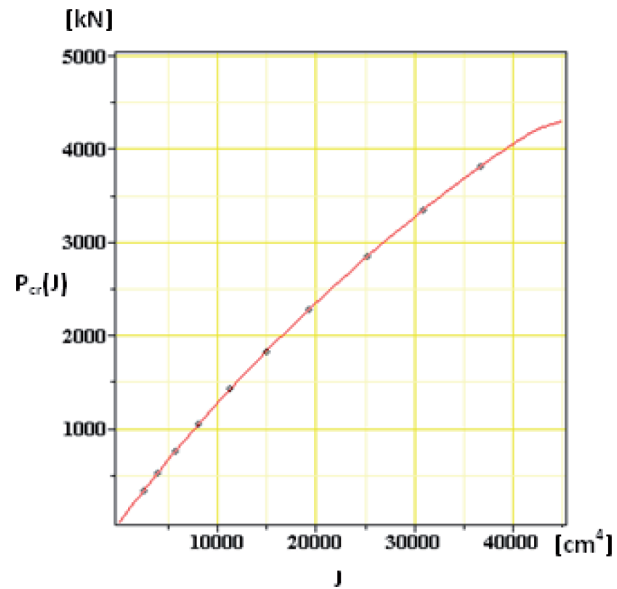


Fig. 7. Polynomial approximations for the critical force vs. inertia moment.
Rys. 7. Wielomianowa aproksymacja siły krytycznej w funkcji momentu bezwładności

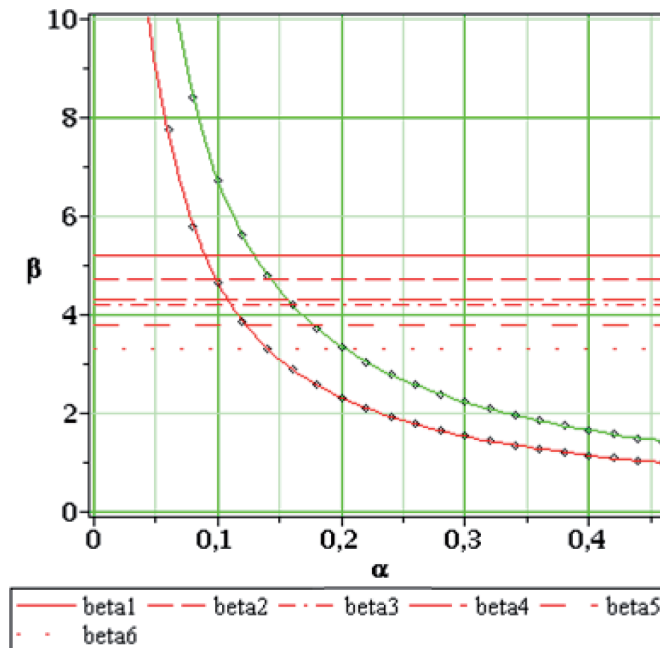


Fig. 8. Reliability indicators for the 2D FEM model of the steel multi-span frame.
Rys. 8. Wskaźniki niezawodności dla dwuwymiarowego modelu MES wieloprzęsłowej ramy stalowej

values of this indicator in order to make a quantitative verification of the safety region. Similarly as before, the random fluctuations in Young modulus are more dangerous to this structure than the fluctuations of inertia moments of the columns (with the same magnitude). This structure is significantly more sensitive to the random fluctuations since unconditional safety for $E=E(\omega)$ is obtained for $\alpha(E) \leq 0.08$ and for $\alpha(J) \leq 0.12$ in the case of $J=J(\omega)$. Now reliability indices tend more apparently and much faster to 0 together with $\alpha \rightarrow \infty$. The safety margin in-between 1 and 50 years exploitation is about few hundreds in both coefficients of variation, so that practically is really small.

4.4. CYLINDRICAL SHELL STABILITY

The last computational example serves for a demonstration of the RFM approach to the large scale problem also with initial Gaussian uncertainty. According to the practical needs of the underground structures design, a fundamental issue is the optimal determination of the structure thickness. Since the entire structure is a small tank serving as a water reservoir or the fluid phase waste container manufactured from the polymers injected into a solid form by the rotation technique of the cylindrical part and welding of both ends, the arbitrary constant thickness is usually adopted. The following data characterize this structure: (a) Young modulus $E=1400$ MPa, (b) Poisson ratio $\nu=0.35$,

(c) mass density equivalent to 15 kN/m^3 , (d) total number of nodal points – 4989, (e) total number of 4-noded shell finite elements with Coons automatic meshing algorithm – 4752, (f) structure height – 3.0 m, (g) cylinder radius – 1.8 m, (h) mean value of its thickness – 0.032 m (a discretization is shown in Fig. 9). The upper cover has a spherical character with the height equal to 0.10 m and this point is 1.50 m below the ground surface, the bottom plate is simply supported on its entire lower surface. The whole structure is modeled as an empty container subjected to all external loads as subsoil pressure, dead load, snow and vehicle uniform loadings, specified according to the additional Eurocodes. The stability analysis performed also by using the FEM engineering system ROBOT deals with this non-uniform shape of the external load, where its critical magnitude is a subject of this computational study. The probabilistic moments are determined via the RFM approach implemented in the system MAPLE, where the structural polynomial response between this critical magnitude and structural thickness is finally included into the stochastic perturbation procedure. Let us note here that material properties are usually treated as random or even stochastic for the structural members manufactured from composites and/or the reinforced plastics; geometrical parameters are randomized accidentally but similarly to the previous analyses we randomize both thickness and Young modulus [13,14]. Polynomial approximation given in Fig. 10 below is completed from 23 points probing procedure around the mean value of the structural thickness specified on the horizontal axis. The RFM is based on uniform subdivision of the computational domain and the least squares fitting procedure returns here the satisfactory, smooth response function with no end oscillations even for the equal unit weights. Of course, the RFM is applied here by using global version of this method since the thickness is designed as constant and the single parameter results from this analysis (unlike for stresses or displacements, where local formulation would be necessary). Unlike in previous examples, the response function is monotonously increasing for the given thickness variability interval (according to initial predictions) and is convex everywhere.

The reliability indicators visualized in Fig. 11 demonstrate a large difference between the uncertainty in Young modulus and inertia moment (practically thickness). The unconditional safety region (independent from the chosen reliability class) is noticed for $\alpha(J) \leq 0.14$ (upper curve); in the case of $E = E(\omega)$ is significantly smaller, i.e. $\alpha(E) \leq 0.05$ (almost deterministic problem). It shows that the optimization of this structure needs to be processed by an additional increase of Young modulus rather (thanks to the usage of high density or simply reinforced polymers, for instance) than by enlarging of the shell thickness. As it can be expected from this analysis, $\beta = \beta(E, \alpha)$ tends to 0 very fast (almost within the given variability interval). Is it also clear that the unconditional failure is obtained for $\alpha(E) > 0.075$ and, separately, for $\alpha(J) > 0.24$ (almost three times larger than before). Let us note that it would be of some practical importance to consider the uncertainty in the external loads – more extensive vehicle motion on the surface or higher subsoil above this container. Finally, it should be underlined that an application

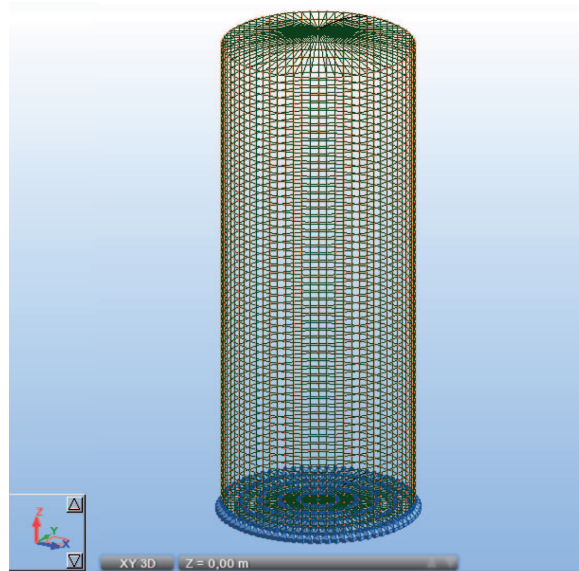


Fig. 9. FEM model of the cylindrical shell structure.
Rys. 9. Model MES cylindrycznej struktury powłokowej

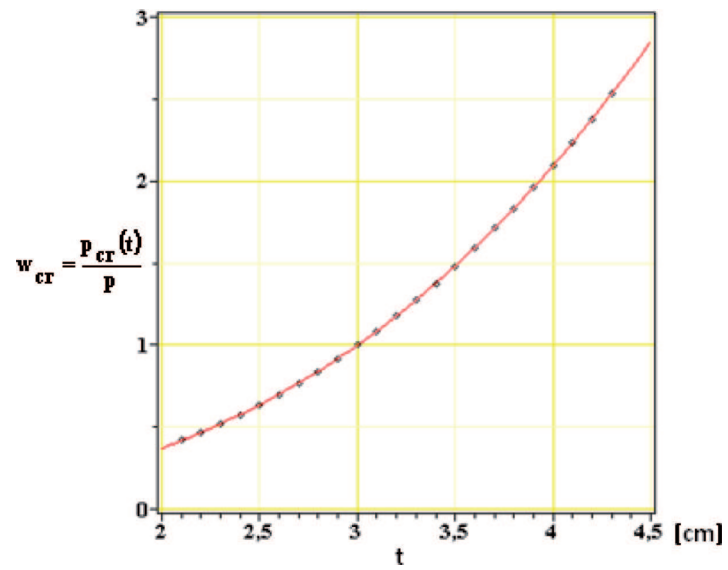


Fig. 10. Polynomial approximation for the shell critical pressure vs. its thickness.
Rys. 10. Wielomianowa aproksymacja dla ciśnienia krytycznego powłoki jako funkcji jej grubości

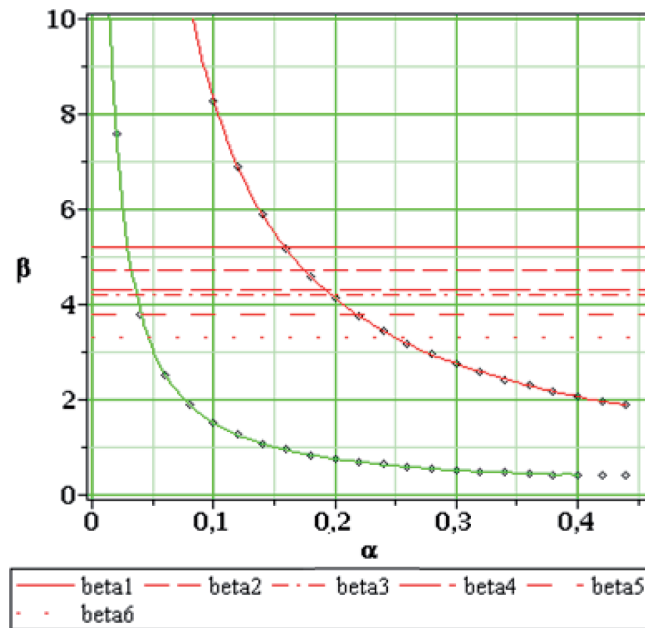


Fig. 11. Reliability indicators for the cylindrical shell FEM model.

Rys. 11. Wskaźniki niezawodności dla modelu MES cylindrycznej konstrukcji powłokowej of the Monte-Carlo simulation for this case study would be extremely time consuming, especially for the situation of the two correlated random input variables; this is not the case of the stochastic perturbation method, where some additional modifications of Eqns (2.6-2.7) are really necessary.

5. CONCLUSIONS

Two alternative computational techniques have been verified in this paper during determination of the reliability indicator of the structures – Monte-Carlo simulation and the generalized stochastic perturbation technique. Even for relatively large values of the input coefficient of variation – up to 0.25 – they both return the same final values of β in the case of the structures examined. It significantly shortens the computational time and allows for the probabilistic analyses of reliability with the use of the commercial FEM packages like ROBOT or ABAQUS in conjunction with some computer algebra system like MAPLE or MAXIMA, for instance. From the methodological point of view it would be essential and the very instructive to re-compute now all indices according to the Second Order Reliability Method to provide a discussion of the FORM and SORM on the basis of the real engineering structures stability.

It is confirmed directly by the computations provided that the higher uncertainty in design parameters, the smaller reliability indicator and, effectively, the larger probability of failure. Although this study has been performed separately for two design parameters

important in steel and, generally, thin-walled structures – Young modulus and inertia moment, the entire perturbation-based approach may be modified accordingly to include a group of correlated or uncorrelated random quantities. Undoubtedly, an interesting problem which can be solved in the next turn, is a temperature-dependent stochastic reliability of especially steel structures – the additional data on thermal fluctuations of all physical parameters of the engineering steels are included into the separate part of Eurocode 3, so that probabilistic Finite Element Method analysis of those special cases in the view of Eurocode must bring qualitatively new results. Such a simulation procedure needs to be important in fire safety designing and verification for the variety of steel structures. There is also no doubt that the stochastic post-critical behavior [15,16] would be of the paramount importance in the stability of complex steel structures, where the initial loss of stability may undergo in quite different paths. Further computational models in that area undoubtedly must obey a simulation of the uncertainty in steel structures connections, sometimes decisive for their overall reliability. However, it needs a preparation of the micro-scale discretization of such structures, which needs a precise knowledge about the probabilistic methods correctness and limitations (like the issues discussed above), as well as decisively more powerful computers and the additional software.

6. ACKNOWLEDGMENTS

The first author would like to acknowledge the Research Grant NN 519 386 636 from the Polish Ministry of Science and Higher Education.

REFERENCES

1. Eurocode: Basis of structural design. BS EN 1990, 2002.
2. R.E. MELCHERS, Structural reliability. Analysis and prediction, Ellis Horwood Limited 1987.
3. I. ELISHAKOFF, Probabilistic methods in the theory of structures, Wiley-Interscience, New York, 1983.
4. I. ELISHAKOFF, Uncertain buckling: its past, present and future, International Journal of Solids and Structures, **37**, 6869-6889, 2000.
5. M. KLEIBER, T.D. HIEN, The Stochastic finite element method, Wiley, 1992.
6. M. KAMIŃSKI, P. ŚWITA, Generalized stochastic finite element method in elastic stability problems, Computers and Structures, **89**, 1241-1252, 2011.
7. M. KLEIBER, Introduction to the finite element method [in Polish], Polish Scientific Publishers, Warsaw-Poznań, 1986.
8. K.J. BATHE, Finite element procedures, Prentice Hall, 1996.
9. M. KAMIŃSKI, Potential problems with random parameters by the generalized perturbation-based stochastic finite element method, Computers and Structures, **88**, 437-445, 2010.
10. J.S. BENDAT, A.G. PIERSOL, Random data: analysis and measurement procedures, Wiley, New York, 1971.
11. R.M. JONES, Buckling of bars, plates and shells, Bull Ridge Publishing, Blacksburg, Virginia, 2006.

12. S.P. TIMOSHENKO, J.M. GERE, Theory of elastic stability, McGraw-Hill, New York, 1961.
13. V. PAPADOPOULOS, V. CHARMPIS, M. PAPADRAKAKIS, A computationally efficient method for the buckling analysis of shells with stochastic imperfections, Computational Mechanics, **43**, 687-700, 2009.
14. V. PAPADOPOULOS, G. STEFANO, M. PAPADRAKAKIS, Buckling analysis of imperfect shells with stochastic non-Gaussian material and thickness properties, International Journal of Solids and Structures, **46**, 2800-2808, 2009.
15. A. STEINBÖCK, X. JIA, G. HÖFINGER, H. RUBIN, H.A. MANG, Remarkable postbuckling paths analyzed by means of the consistently linearized eigenproblem, International Journal in Numerical Methods in Engineering, **76**, 156-182, 2008.
16. B.W. SCHAFER, L. GRAHAM-BRADY, Stochastic post-buckling of frames using Koiter's method, International Journal of Structural Stability and Dynamics, **6**, 333-358, 2006.
17. Maplesoft, division of Waterloo Maple Inc.
18. Autodesk® Robot™ Structural Analysis Professional.

MODELOWANIE NIEZAWODNOŚCI W PEWNYCH ZAGADNIENIACH STATECZNOŚCI
SPRĘŻYSTEJ Z WYKORZYSTANIEM UOGÓLNIONEJ STOCHASTYCZNEJ METODY
ELEMENTÓW SKOŃCZONYCH

S t r e s z c z e n i e

Zasadniczym problemem omawianym w tej pracy jest zastosowanie Uogólnionej Stochastycznej Metody Elementów Skończonych opartych na metodzie perturbacji stochastycznej do wyznaczania wskaźników niezawodności w przypadku stateczności konstrukcji budowlanych pracujących w zakresie sprężystym. Wskaźnik niezawodności jest modelowany zgodnie z definicją podaną w normie Eurokod odpowiednią dla analizy niezawodności pierwszego rzędu, a obliczony dzięki zastosowaniu rozwinięcia wszystkich funkcji stanu w szereg Taylora ze współczynnikami z uwzględnieniem wyrazów wyższego rzędu. Procedura obliczeniowa jest oparta na jednoczesnym zastosowaniu programu Metody Elementów Skończonych ROBOT oraz systemu algebry komputerowej MAPLE i jest wykorzystana do analizy obciążeń krytycznych w popularnych konstrukcjach inżynierskich takich jak pręt Eulera, dwu i trójwymiarowe modele jedno- i wieloprzęsłowej ramy stalowej, jak również polietylenowy zbiornik podziemny o kształcie cylindrycznym. Porównanie metody perturbacji stochastycznej z techniką symulacji Monte-Carlo w całym zakresie losowej zmienności wykorzystywanych parametrów wejściowych na przykładzie zagadnienia Eulera pokazuje efektywność i ograniczenia zastosowanej metody perturbacji.

*Remarks on the paper should be
sent to the Editorial Office
no later than December 30, 2011*

*Received February 28, 2011
revised version
August 31, 2011*